The Role of Simple Models in Understanding Climate Change

Thomas F. Stocker
Climate and Environmental Physics
Physics Institute, University of Bern
Sidlerstrasse 5, CH–3012 Bern, Switzerland
stocker@climate.unibe.ch

In: *Continuum Mechanics and Applications in Geophysics and the Environment.*
B. Straugham, R. Greve, H. Ehrentraut, Y. Wang (eds.)
Springer Verlag, pages 337-367 (2001).

March 18, 2002

Abstract

The study of the Earth System has a long tradition of using simplified models to achieve a quantitative understanding of processes that are responsible for climate change. The examples of the carbon cycle and the ocean circulation in shaping past and future climate evolution are discussed here and the development from early box models to dynamical models of reduced complexity is reviewed. The latter models are beginning to play a significant and increasing role on our way to a better understanding of the Earth System.

1 Introduction

Quantitative climate research requires numerical models. A common philosophy is to develop a single comprehensive model and strive for maximum resolution and number of represented processes. This implies that one uses general circulation models of the atmosphere, and the ocean which are then coupled to model components of biogeochemical cycles in the ocean and the terrestrial biosphere. There only very few research centers worldwide who can afford to develop such models which are intensive in human resources and computers. More importantly, the current computer power precludes in-depth sensitivity studies and integrations that extend over many hundreds of years.

Complementary to this, simplified models have been developed over the last few years and it was demonstrated that these models are capable of correctly simulating important aspects of the climate system. This class of models has been referred to recently as *Earth System Models of Intermediate Complexity* and they have caught the attention of numerous research groups internationally. These simplified, or low-order models, solve only a reduced number of dynamical equations of the Earth System. For example, some

aspects of the large-scale ocean circulation are well described by solving zonal averages of the primitive equations. Similarly, on time scales of centuries and up, processes of the atmosphere may be approximated as being in energy balance with respect to those in the ocean. Such models are extremely efficient and can be used to explore systematically the parameter space.

Beyond this specific example there are a number of similar approaches which include further components of the climate system such as the vegetation cover or the marine carbon cycle. Together, these models form a *hierarchy* of climate models. Quantitative testing of hypotheses regarding the operation of the climate system in the past requires the full climate model hierarchy. The same models are also used to assess how the climate will evolve in the future. The extent to which these models can realistically describe past changes in the climate system is thus of immediate relevance to the degree of confidence with which we can make predictions about climate in an atmosphere that will contain twice as much CO_2 as has existed anytime during the last 420,000 years in less than a century.

The purpose of this contribution is to discuss a few examples in which simplified climate models have been successfully used to further our understanding of the complex processes in the climate system. An important ingredient of climate modeling is the constant "communication" between model results and paleoclimatic reconstructions in the form of proxy data and direct observations. While this poses generally a big challenge to simplified models, it is also a source of constant refinement of mode set up and parameterisation.

2 Ocean and abrupt climate change

2.1 Climatically relevant ocean circulation types

The climate system consists of four major components. These are the atmosphere, the cryosphere, the terrestrial biosphere and the ocean. This subdivision is somewhat arbitrary and other approaches, e.g. according to the relevant cycles of heat, water and tracers, are equally valid. The terrestrial biosphere and the cryosphere (ice sheets) are important drivers of climate change. The former has a strong influence on the hydrological cycle and the albedo (Crowley & Baum 1997) whereas the ice sheets are mainly influencing atmospheric circulation and the surface radiative balance through the ice-albedo feedback (see Crowley & North 1991). Rapid ice flow, however, can act as a strong perturbation to the ocean circulation if this ice is discharged into the ocean and produces large amounts of meltwater (MacAyeal 1993).

Here, we focus on the ocean which appears to play an important role in the framework of abrupt climate change. The ocean is an important component of the climate system because it covers 70% of the Earth's surface. Considering ocean and atmosphere as the only components that are relevant for climate changes on time scales of less than 10^4 years, the ocean contains 95% of water and 99.9% of the heat content. However, it is the dynamics that is essential in providing a mechanism for abrupt change.

The present description of ocean circulation types is very basic and concerns only the

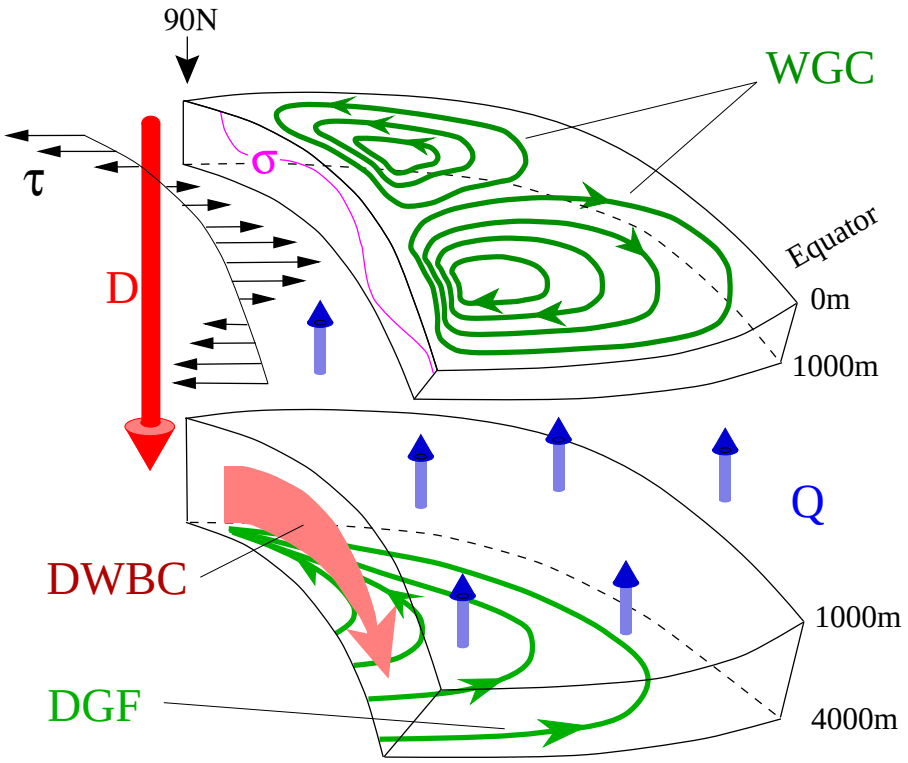

Figure 1: Schematic view of the different types of steady-state circulations in a sectorial ocean basin extending from the equator to the pole with a longitudinal extent of roughly 60°. Wind stress τ drives a *wind driven gyre circulation* (WGC) which shows western intensification due to the curvature of the rotating Earth. τ also causes Ekman upwelling in the northerly and Ekman downwelling in the southerly upper layer giving a near-surface isopycnal surface σ its typical shape: the isopycnal is shallow below the subpolar gyre and deep below the subtropical gyre. A source of newly formed deep water, D, feeds the deep ocean in which a *deep western boundary current* (DWBC) develops from which the *deep geostrophic flow* (DGF) of the interior is derived. DGF flows northward to conserve potential vorticity while slowly upwelling. This results in a vertical mass flux Q that closes the flow. In reality, $Q < D$ in this sector and the DWBC is crossing the equator setting up a global circulation [From Stocker 1999].

most important, large-scale flows; here we follow Stocker (1999). The major processes that govern the dynamics are the action and regional distribution of momentum and buoyancy fluxes at the ocean's surface, the Earth's rotation and the presence of ocean basin boundaries. Four large-scale circulation types characterize the flow in an ocean basin (Fig. 1). The general circulation is forced by the input of momentum through surface wind stress τ and by the flux of negative buoyancy, indicated by the vertical arrow D and uniform upwelling Q (Fig. 1). The surface wind stress forces the wind-driven geostrophic circulation (WGC) which is intensified at the western boundary and forms the subtropical and the subpolar gyres. In the interior of the ocean basin, there is a balance between the pressure gradients and the Coriolis forces acting on the moving fluid. Western intensification, on the other hand, is a consequence of the spherical shape of the rotating Earth and frictional effects in the fluid and at the basin boundaries (Stommel 1948; Pedlosky 1996).

Winds blowing over the surface of the ocean lead to divergent (Ekman upwelling) or convergent (Ekman downwelling), frictionally driven flows and change the local depth of

the near-surface isopycnals σ (lines of constant density) which set up horizontal pressure gradients with associated geostrophic flows. These flows are responsible for the fact that the wind-driven gyres do not extend all the way to the bottom but are compensated by sloping isopycnals in the top few hundred meters. In other words, the geostrophic velocities exhibit a vertical structure, and the wind-driven circulation remains confined to the top few hundred meters of the water column (Pedlosky 1996).

Turning now to the deep circulation, the source D feeds the deep western boundary current (DWBC) which flows southward and leaks into the deep interior where the geostrophic flow (DGF) is directed polewards at all latitudes. The DGF recirculates into the source area of the DWBC. There is a cross-interface mass flux Q upwelling into the upper 1000 m which supplies the mass lost due to D in the upper layer.

There are only a few locations in the ocean where new deep water is being formed. These are the Greenland-Iceland-Norwegian Seas in the north and the Weddell Sea in the south and a few other, minor sites (Marshall & Schott 1999). The dynamics of a fluid moving on a rotating sphere dictates that also the deep flow is confined to western boundary currents (Stommel 1958; Stommel & Arons 1960). In the present ocean, the northern source is strong enough so that the current crosses the equator and penetrates eventually into the southern ocean. There, it mixes with the deep waters from the Weddell Sea and flows into the Indian and Pacific oceans where broad upwelling occurs. The global structure of the deep water paths was already suggested by the late Henry Stommel (1920–1992) in a pioneering paper (Stommel 1958); the return flow in the thermocline, preferentially via the 'warm water route' around Africa (de Ruijter *et al.* 1998), was first described by Gordon (1986). This global flow subsequently became known as the 'conveyor belt' (Broecker 1987; Broecker 1991), but the structure is far more complicated than a simple ribbon spanning the globe (Schmitz 1995).

Evaluations of the radiation balance at the top of the atmosphere show that the ocean-atmosphere system must transport heat towards the high latitudes where there is a net loss of energy over one year (Trenberth & Solomon 1994). About half of that heat is carried by ocean currents (Macdonald & Wunsch 1996). In contrast to the other ocean basins, the meridional heat transport in the Atlantic Ocean is northward at all latitudes. Evaluation of oceanographic observations (Hall & Bryden 1982) as well as model simulations (Böning *et al.* 1996) indicate that the meridional heat transport in the Atlantic is primarily due to the meridional overturning circulation which carries warm near-surface waters northward and cold deep water southward. This is the deep circulation of the ocean that is driven by surface buoyancy fluxes and is referred to as the "thermohaline circulation", short THC (Warren 1981). The wind-driven, near-surface circulations in the Atlantic do not transport significant amounts of heat polewards. The THC in the Atlantic is also often referred to as the "nordic heat pump".

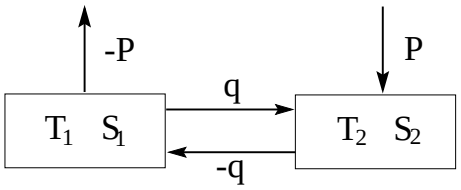

Figure 2: A 2-box version of the world ocean. Water is exchanged between a low (T_1, S_1) and a high-latitude box (T_2, S_2) at rate q. The cycle of freshwater is closed through an "atmosphere" in which precipitation P is negative in the low and positive in the high latitudes, i.e. northward water transport. [From Marotzke (1990)]

3 Lessons from simplified models

3.1 Box models

The late Henry Stommel, whose fundamental contributions to the understanding of the general circulation of the world ocean were already outline above, formulated a simple 2-box model for the deep circulation (Stommel 1961). His goal was to investigate whether the interaction between meridional density differences set up at the ocean surface by the conditions of the atmosphere and the deep circulation which tries to erase these differences could give rise to some interesting dynamics. The surprising result was that such a simple flow system could exhibit multiple equilibria, provided the response time of the ocean's sea surface to heat anomalies is different to that responding to freshwater anomalies.

This feature is best illustrated in the simplified version of the Stommel box model presented by Marotzke (1990). The existence of multiple equilibria in the ocean can be demonstrated quantitatively in the complete hierarchy of ocean models and is thus a robust result of the models, but the basic insight of the mechanisms at work comes from simplified models.

Marotzke's model consists of only two boxes: a box representing the low-latitudes with warm temperatures and one for the high latitudes where the temperatures are cold (Fig. 2). The temperature difference, ΔT, between the boxes is held fixed assuming that it is determined by strong coupling to the atmosphere. We now consider the salt balance which is given by

$$\dot{S}_1 = |q| \cdot (S_2 - S_1) + P \ , \quad \dot{S}_2 = |q| \cdot (S_1 - S_2) - P \quad , \tag{1}$$

where q is a meridional water transport, P denotes net precipitation (in salt units), and S_1 and S_2 are the salinities in the low and high-latitude boxes, respectively (Fig. 2). The transport is assumed to be proportional to the density difference between the boxes:

$$q = k \cdot (\rho_2 - \rho_1) = k\alpha \cdot (T_2 - T_1) + k\beta \cdot (S_2 - S_1) \quad , \tag{2}$$

where we have made use of the equation of state for sea water:

$$\rho = \rho(T, S, p) \approx \rho_0 \cdot \Big(1 + \alpha \cdot (T - T_0) + \beta \cdot (S - S_0) + \gamma \cdot (T - T_0)^2\Big) \quad , \tag{3}$$

with $T_0 = 0°\mathrm{C}$, $S_0 = 35\,\mathrm{psu}$, $\rho_0 = 1028.1\,\mathrm{kg/m^3}$, $\alpha = -5.26{\cdot}10^{-5}\,\mathrm{K^{-1}}$, $\beta = 7.86{\cdot}10^{-4}\,\mathrm{psu^{-1}}$ and $\gamma = -6.6 \cdot 10^{-6}\,\mathrm{K^{-2}}$, see Gill (1982). Neglecting now the non-linear term in (3) we

obtain steady states of (1) according to

$$\Delta S = \begin{cases} -\dfrac{\alpha\Delta T}{2\beta} \pm \sqrt{\left(\dfrac{\alpha\Delta T}{2\beta}\right)^2 - \dfrac{P}{k\beta}} \quad , \quad q > 0 \quad , \\ \\ -\dfrac{\alpha\Delta T}{2\beta} + \sqrt{\left(\dfrac{\alpha\Delta T}{2\beta}\right)^2 + \dfrac{P}{k\beta}} \quad , \quad q < 0 \quad . \end{cases} \tag{4}$$

Substituting the positive non-dimensional quantities

$$\delta = -\frac{\beta\Delta S}{\alpha\Delta T} \ , \quad E = \frac{\beta P}{k(\alpha\Delta T)^2} \quad , \tag{5}$$

into 4 we obtain

$$\delta = \begin{cases} \frac{1}{2} \pm \sqrt{\frac{1}{4} - E} \quad , \quad q > 0 \quad , \\ \\ \frac{1}{2} + \sqrt{\frac{1}{4} + E} \quad , \quad q < 0 \quad . \end{cases} \tag{6}$$

We note that for a direct circulation (cold waters are sinking) $q > 0$. Equation (6) implies that for $E < 0.25$ there are two equilibrium states with a direct circulation, and one equilibrium state with an indirect circulation. It can be shown that the state with the intermediate δ is not stable. When E increases, i.e. precipitation in the high-latitude box becomes stronger, the number of equilibrium states is reduced to one for $E > 0.25$. For large P or small ΔT, i.e. $E > 0.25$, only the indirect circulation is a steady state, in other words the circulation has changed direction. The effect of salinity on density is now dominant and waters are sinking in the low-latitude box.

The reason for multiple equilibria lies in the physics of the different components of the surface buoyancy flux. Sea surface temperature (SST) anomalies create local heat flux anomalies that tend to erase the SST anomalies effectively since fluxes are essentially proportional to the temperature difference between the ocean and the atmosphere. Temperature anomalies therefore have a short lifetime; this is accounted for by setting ΔT constant in the above box model. Sea surface salinity (SSS) anomalies, on the other hand, have no influence on freshwater fluxes nor on heat fluxes implying that SSS anomalies will have a much longer residence time on the ocean surface. In the box model, this is acounted for by the fact that P is independent of S; in ocean general circulation models one selects "mixed boundary conditions" to mimick this effect (Rooth 1982).

Henry Stommel concludes his seminal paper by the following words:

> "One wonders whether other, quite different states of flow are permissible in the ocean or some estuaries and if such a system might jump into one of these with a sufficient perturbation. If so, the system is inherently fraught with possibilities for speculation about climatic change."
>
> *Henry Stommel, 1961*

These early insights were forgotten for another 20 years until marine sediment cores and ice cores from the Greenland ice sheet were analyzed in sufficiently high temporal resolution. At the same time, in the mid eighties, F. Bryan showed multiple equilibria of the THC in a 3-dimensional ocean model (Bryan 1986). This finally convinced researchers that the ocean takes a central and *active* role in shaping the climate and its evolution.

3.2 Simplified dynamical models

It has always been tempting to reduce the complexity of the equations that govern atmospheric and oceanic motions (Navier-Stokes equations in a rotating frame) such that fundamental insights can be extracted. One such reduction is (2) but one notices that further reduction would restrict the deegrees of freedom of a system to such an extent that its behaviour may become trivial. The art is therefore to construct a hierarchy of models.

This approach has proven very successful in classical climate dynamics in which global-scale aspects were of interest. A famous reduction are the energy balance models of Sellers (1969) and Budyko (1969). In the 70ies various types of energy balance models emerged (see e.g. North *et al.* (1981) for an overview) which were used as early tools to assess the problem of global warming. Turning to the large climatic changes of glacial-interglacial cycles, simple energy balance models were no longer sufficient and the effect of land and ice masses on the radiative balance needed to be incorporated (Galleé *et al.* 1991). This was done by zonally averaging a simplified, quasi-geostrophic atmosphere and introducing a number of parameterizations which represented land surface processes.

With the recognition that the ocean's thermohaline circulation was important to understand climate change (Broecker *et al.* 1985), there was an apparent lack of simplified, yet dynamical models of the ocean circulation. A first step was made by Marotzke *et al.* (1988) who zonally averaged the basic equations in a rectangular basin. These authors noted that, unlike in the idealized atmosphere, in the ocean a problem arises due to meridional basin boundaries. At these boundaries, zonal pressure differences can be supported which drive – via the Coriolis force – ocean currents. They proposed to replace this mechanism by fricion and found that a reasonable meridional circulation can be obtained, albeit at unrealistically high values of friction. Wright & Stocker (1991) presented a first solution to this problem by arguing that the zonal pressure difference is related to the meridonal pressure gradient. This closure assumption allowed them to formulate a dynamically consistent model of the deep circulation. It was shown later, that based on the theory of oceanic boundary currents, one could derive a more rigorous, non-local closure formulation which shows remarkable agreement with results from 3-D ocean models containing the complete large-scale dynamics (Wright *et al.* 1998).

The model was then extended to two meridional basins, "Pacific" and "Atlantic", which were connected at their southern ends (Stocker & Wright 1991b). Forcing the ocean model with observed zonally averaged Pacific and Atlantic sea surface temperatures and salinities, a circulation reminiscent of the "global conveyor belt" was obtained (Fig. 3). Although highly simplified, such a model produces strikingly realistic distributions of temperature and salinity in both ocean basins. The unstable isotope of carbon (^{14}C, half live 5730 years) is an important tracer to check time scales in ocean models. Fig. 3 shows the steady-state distribution of ^{14}C in both basins and comparison with observations indicate good agreement. These results encouraged further studies using this type of models.

By completing it with an energy balance model of the atmosphere (Stocker *et al.* 1992) and a seasonal cycle (Schmittner & Stocker 2001), a coupled model was constructed which filled the gap between the useful energy balance models and the comprehensive

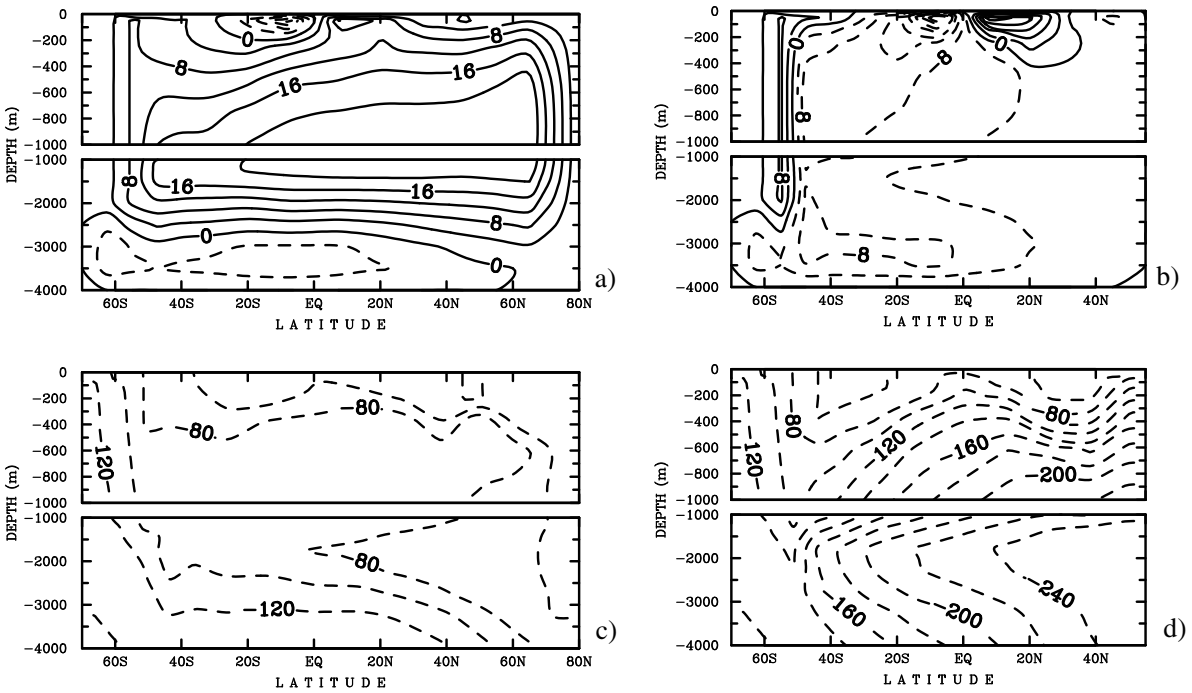

Figure 3: The steady state of the overturning stream function in the Atlantic (a) and the Pacific (b). The water mass distribution is best evidenced by the distribution of radiocarbon in both basins (c, Atlantic; d, Pacific). [From Stocker & Wright 1996]

3-dimensional coupled climate models. Such a model proved to be extremely efficient and model simulations extending over thousands of years were feasible. More importantly, these models could be used for a first check of parameter space to identify new mechanisms or solution properties that could be later verified using comprehensive 3-D models. By such an approach, the simplified models can actually guide the more expensive models into areas worthy of further research.

In the last few years this model philosophy has become quite popular and the applications fall into three groups: (i) basic, fluid-dynamics motivated studies (e.g., Quon & Ghil 1994, Saravanan & McWilliams 1995); (ii) extensive parameter sensitivity studies for specific ocean and climate problems (e.g., Wright & Stocker 1992, Schmittner & Stocker 1999, Knutti *et al.* 2000); (iii) long-term simulations including vegetation and biogeochemical cycles (e.g., Claussen *et al.* 1999, Joos *et al.* 1999, Marchal *et al.* 2000).

This type of ocean model was recently coupled a statistical dynamical formulation of the atmosphere in which meridional and zonal transports are parameterised in terms of surface temperature (Petoukhov *et al.* 2000). The model is tuned to present-day observations and appears to be able to also simulate other climate states such as the last glacial maximum (Ganopolski *et al.* 1998).

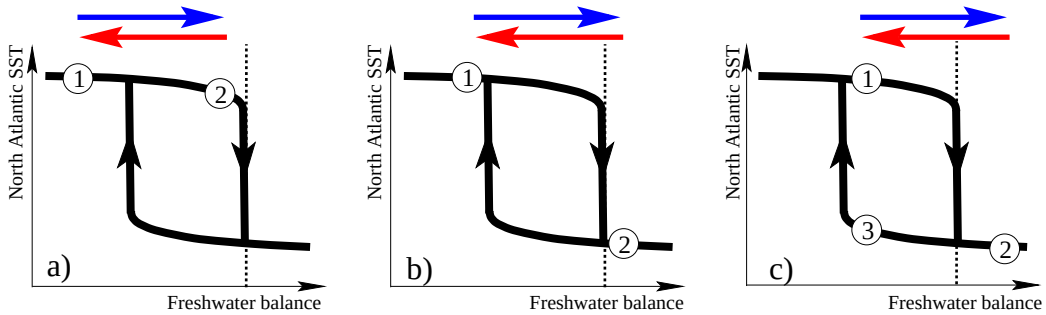

Figure 4: The ocean-atmosphere system is a non-linear physical system that can exhibit hysteresis behaviour (Stocker & Wright 1991a). A given perturbation (indicated by the horizontal arrows) in the freshwater balance of the North Atlantic (precipitation+runoff–evaporation) causes transitions from an initial state ① to states ② and/or ③. Three structurally different responses are possible depending on whether threshold values (dashed line) are crossed **a:** Linear, reversible response. **b:** Non-linear, reversible response. **c:** Non-linear, irreversible response. [From Stocker & Marchal 2000]

3.3 Hysteresis uncovered

Experiments with simplified ocean circulation and climate models have helped to discover and understand some fundamental features of the climate system. One such is the hysteresis behaviour of the atmosphere-ocean system.

The freshwater balance in the North Atlantic governs the strength of the thermohaline circulation: in high latitudes surface waters are cooled and lose buoyancy. On the other hand, there is excess precipitation which increases buoyancy. The competition between these two effects, which activate very different feedback mechanisms in response to a change, gives rise to the possibility of large changes in the thermohaline circulation. Such changes are due to the existence of multiple equilibria of the THC as already shown by Stommel (1961) and explained in the box model above. This implies that the thermohaline circulation, like many nonlinear physical systems, may exhibit hysteresis. This was first shown by Stocker & Wright (1991a) using a simplified model: for certain values of a control variable the system may have more than one permissible values of a climate variable (Fig. 4). Numerous studies using a variety of models have demonstrated the existence of hysteresis (Mikolajewicz & Maier-Reimer 1994; Rahmstorf 1995) and we conclude that this is a robust property of the coupled atmosphere-ocean system.

The existence of hysteresis implies various different possibilities how the system can respond to changes in the control variable. More freshwater in the sinking regions reduces the THC. The system is stable and reacts in a linear fashion as long as threshold values are not crossed (Fig. 4a). An abrupt change with an amplitude that no longer scales with the perturbation occurs if a threshold or critical value is crossed (Fig. 4b). If the initial state of the ocean-atmosphere system is a unique equilibrium, the system jumps back to the original state once the perturbation has ceased: the abrupt change is reversible. However, if other equilibria exist, the perturbation causes an irreversible change (Fig. 4c). Hysteresis is well known in climate models and considered a robust feature, but its structure is highly model dependent. A burning question is: where are we now on the hysteresis, what is its structure and how close is the threshold?

Without our detailed knowledge of past climate change and with its frequent occurrence

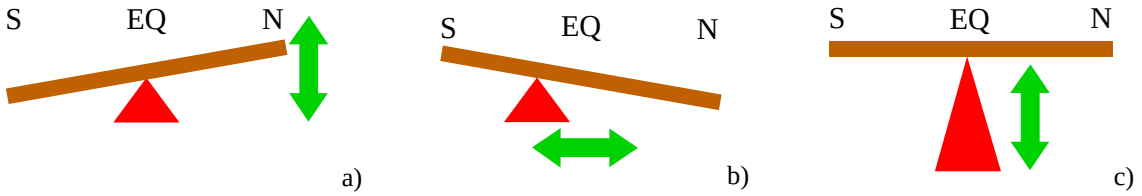

Figure 5: Simple mechanical analog of three different types of behaviour of the climate system as a response to perturbations (arrows). **a:** Perturbations in the northern high latitudes (e.g. meltwater from the continental ice sheets) trigger transitions between different states of the thermohaline circulation in the North Atlantic. Through the effect of the meridonal heat flux in the Atlantic, the amplitudes of climate signals are large in the region around the North Atlantic and are weak and of opposite sign in the south. This is the typical inter-hemispheric seesaw forced in the northern North Atlantic reghion. **b:** Perturbations in the tropical region (e.g. hydrological cycle feeding into the Hadley cell) cause transitions between different states of the thermohaline circulation in the North Atlantic with effects identical to (a). This is analogous to a seesaw, whose motion is forced by changes of the position of the hinge point. **c:** Perturbations in the tropical region lead to parallel changes in northern and southern hemispheres. Here, the seesaw is locked and changes synchronous and in phase everywhere. [From Stocker 1998]

of abrupt swings in the North Atlantic climate, we would not be convinced that abrupt climate change is of more than just academic interest. The ice core records in Greenland (Dansgaard *et al.* 1993; Alley 2000), and many other paleoclimatic archives, however, tell a compelling story of dramatic changes that involved temperature changes in Greenland in excess of 15°C (Lang *et al.* 1999) and up to 5°C (Sachs & Lehman 1999) in the subtropical Atlantic within a few decades. Currently, the only theory that is consistent with most of the regional and interhemispheric paleoclimatic evidence is that these changes are associated with large and rapid changes of the Atlantic THC.

3.4 The bipolar seesaw

A remarkable prediction of simplified models is the so-called "bipolar seesaw" (Broecker 1998; Stocker 1998), a mechanism which explains how climatic changes in both hemispheres are linked during abrupt changes. Crowley (1992) suggested that an active thermohaline circulation actually cools the southern hemisphere basing his arguments on a box model. The effect could be clearly reproduced in the simplified models (Stocker *et al.* 1992; Stocker *et al.* 1992) and later also with coupled AOGCMs (Schiller *et al.* 1997; Manabe & Stouffer 1997). This suggested that a collapse of the THC in the Atlantic, which leads to a cooling in the north, would simultaneously result in a warming in the south. While the cooling in the north is abrupt, the heat capacity of the large volume of water in the south is responsible for a much slowerwarming. These models therefore predict that a fingerprint of a complete shutdown of the Atlantic THC would be a warming in areas influenced by the southern ocean. In particular, the prediction would be that with the abrupt coolings and warmings registered in Greenland during the glacial (Dansgaard/Oeschger events, Dansgaard *et al.* 1993) one should be able to observe warmings and coolings in antiphase with the north. As we will discuss below, that is precisely what the high-resolution paleoclimatic records tell us.

4 Past Abrupt Climate Changes

4.1 North-south connection during the glacial

Much progress in paleoclimatic studies of the last few years was due two reasons: (i) a general increase in resolution of the marine and ice core records and (ii), a new technique with which paleoclimatic records from very distant areas can be synchronised, i.e. their changes are put on a common, but not necessarily absolute, time scale. The first results from to an improvement of precision and a significant reduction in sample size required for these measurements. The second is due to the fact that gases in the atmosphere have a mixing time of a few years which is short compared with the typical time scale of climate changes. However, synchronisation would not be possible if all gas constituents remained constant over time. It is thus very fortunate that the atmospheric CH_4 concentration is increasing by about 50% for every D/O event during the last glacial (Chappellaz *et al.* 1993; Dällenbach *et al.* 2000) producing a clock which can be read in the ice cores from both Greenland and Antarctica. This technique was successfully applied to the deglaciation (Blunier *et al.* 1997) and the late glacial (Blunier *et al.* 1998) and it was shown, that during abrupt coolings and warmings in Greenland, the climate evolved with opposite trends in Antarctica.

This is shown in Fig. 6. Events 8 and 12 are followed by longer cooling events and are accompanied by changes in Antarctica. For both of these, the slow warming in Antarctica begins about 2000 years before the abrupt warming in the north (events 8 and 12). At the time of the abrupt transition to the interstadial in the north, cooling starts in the south (events A1 and A2). No distinct changes in Antarctica are detected during the shorter D/O events 5, 6 and 9, 10. For events 7 and 11, there may be an indication of changes similar to A1 and A2 but smaller in amplitude. The D/O events (except 9) are coeval with increased values of atmospheric methane, but there is no correlation with events A1 and A2 suggesting that humid conditions in tropics may have been more strongly influenced or even caused by climate changes of the northern hemisphere.

Marine records also exhibit series of abrupt changes in composition: layers with abundant coarse-grain lithic fragments indicate detrital material transported from the bedrock underlying the great ice sheets to the North Atlantic by calving icebergs (Heinrich 1988). These calving events, later termed "Heinrich Events" (H-event) occurred through surging ice streams which then melted and provided an additional sediment layer. Source areas for the material include the Canadian shield, the Fennoscandian and British ice sheets, but most of the debris material originates from north of Hudson Bay.

At first glance, D/O and H-events seem unrelated. However, Bond & Lotti (1995) showed in a high-resolution marine sediment core from the North Atlantic that smaller layers of ice rafted debris were buried between the prominent Heinrich layers, i.e. such layers also occur during or before D/O events. This is strong indication of a common cause or trigger in the climate system responsible for these changes. The different thickness of the debris layers for D/O and H events suggests that the response of the atmosphere-ocean system depends on the magnitude of the iceberg discharge and possibly involves threshold effects.

The two "fat" D/O events (number 8 and 12, 36 kyr and 45 kyr BP, respectively, see

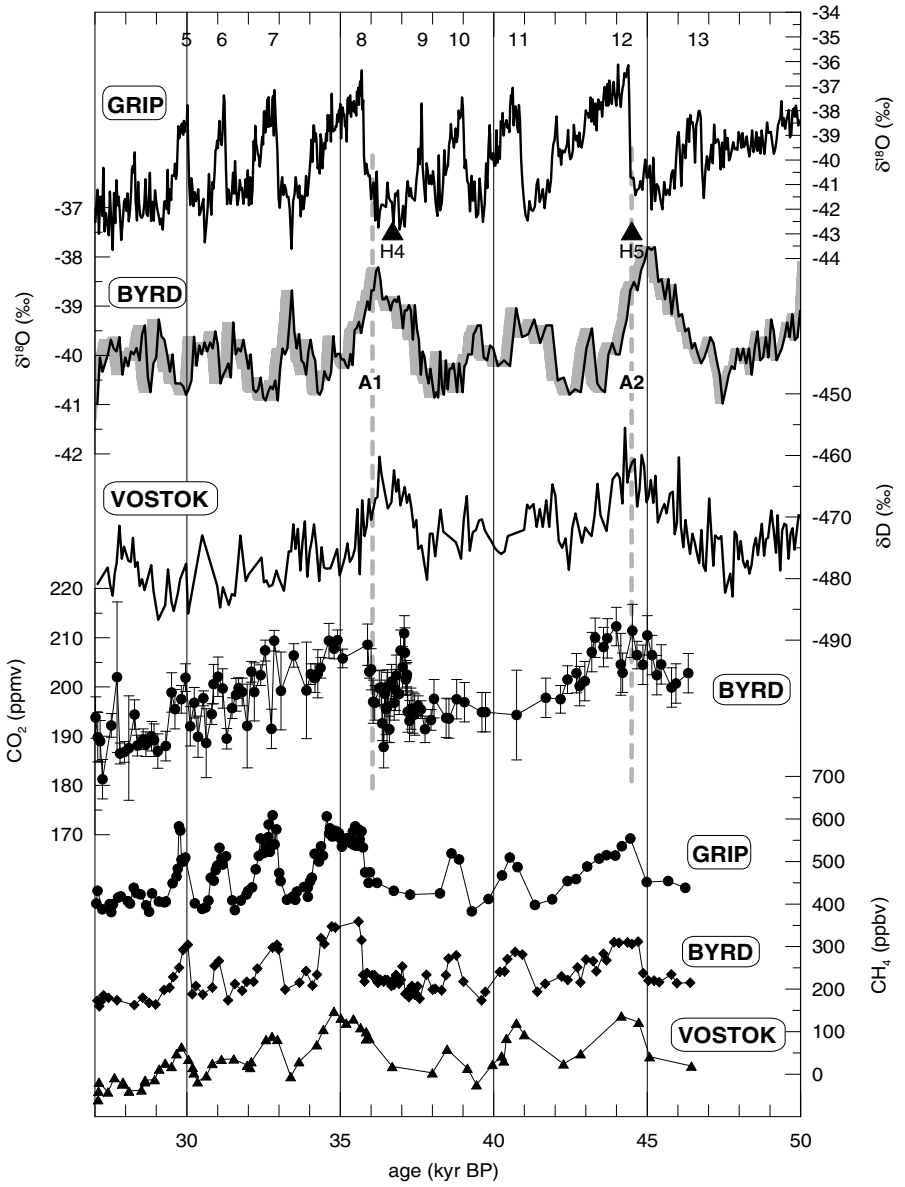

Figure 6: Succession of D/O events 5 to 13 during 27 to 50 kyr BP in the last glacial as seen in Greenland (GRIP) and Antarctic (Byrd Station, Vostok) ice cores. The records are synchronised in time based on high-resolution records of methane (Stauffer *et al.* 1998) (bottom three curves). [modified from Blunier *et al.* (1998)]

Fig. 6) are not only distinct by their duration, but they both occur after a H-event; other, shorter D/O events do not have a preceeding H event. They are clearly associated with climate change derived from the isotopic changes in the Antarctic ice cores (Blunier *et al.* 1998). The warming in the Antarctic record appears steady over about 2 kyr and leads the abrupt warming recorded in the Greenland ice core. At the time of the northern warming, the Antarctic signal indicates a gradual return to colder temperatures over the next 2 kyr.

The above paleoclimatic evidence supports the hypothesis of the bipolar seesaw: a collapse of the THC would stop the nordic heat pump leading to a severe cooling in the northern

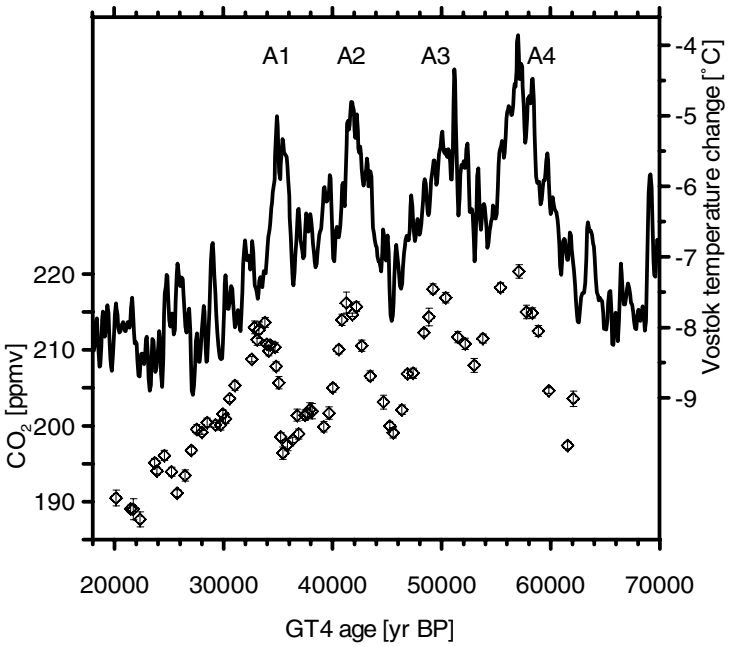

Figure 7: Air temperature record at Vostok (temperature change relative to modern temperature based on measurements of the isotopic composition of the ice). A1 and A2 denote the Antarctic warm events according to Blunier *et al.* (1998). Diamonds denote CO_2 measurements from the Taylor Dome ice core. [From Indermühle *et al.* 2000].

North Atlantic region. As the once active pump has been drawing heat from the southern ocean, this heat is now slowly accumulating in the southern ocean leading to warming.

Further information about the nature of these abrupt events comes from high-resolution CO_2 measurements in ice cores. They indicate that millennial changes of CO_2 during the glacial are less than about 20 ppmv (Indermühle *et al.* 2000). While earlier suggestions that CO_2, much like CH_4, would change during each D/O event could not be confirmed, the CO_2 changes appear correlated to (at least some) Heinrich events and/or the longest and most prominent of the D/O events. Each interstadial A1–A4 in the Antarctic ice core is associated with a relative maximum in CO_2. About 2 kyr before the rapid warming seen in Greenland ice cores, CO_2 appears to rise. This rise roughly coincides with a rise in temperature as indicated by the stable isotopes measured on Antarctic ice cores (Blunier *et al.* 1998; Indermühle *et al.* 2000), although there is still some uncertainty in the ice-age/gas-age difference. Lag correlations indicate a possible lag of the CO_2 increase relative to the warming events A1–A4. CO_2 therefore seems to be more closely linked with the climate changes in the south, than those in the north.

How then, could one explain the warming in the south? Marine sediments contain layers of ice rafted debris at or before each D/O event (Bond & Lotti 1995). This suggests the presence of pools of freshwater which could have acted as triggers of changes in the THC of the Atlantic. Indeed, meltwater discharge to the North Atlantic could be the mechanism to explain the southern warming, because a cooling in the north, caused by the disruption of the nordic heat pump, would lead to a warming in the south. This strong north-south

coupling appears to be present during the few H-events and subsequent "fat" D/O events but weaker or absent during the shorter D/O events (Stocker & Marchal 2000).

In order to test whether the hypothesis of strong north-south coupling during a complete collapse of the Atlantic THC was compatible with the observation of 20 ppm CO_2 change, a simplified physical-biogeochemical climate model was used (Marchal *et al.* 1998; Marchal *et al.* 1999). This model contains a prognostic carbon cycle and simulates atmospheric CO_2. A freshwater perturbation was applied to collapse the THC in the Atlantic which results in a cooling in the north with associated increased uptake of CO_2 through a stronger solubility pump. While the global effect of changes in sea surface temperature remains less than about 5 ppmv with the warming in the south dominating the cooling in the North Atlantic, the combined effect of changes in DIC and alkalinity due to the discharge of the freshwater is an increase of atmospheric CO_2 a few 100 years after the full collapse of the THC in the North Atlantic. The net effect is an increase in atmospheric CO_2 between 7 and 30 ppmv on a timescale of 100 to 2000 years depending on the intensity of the THC change. At the time of abrupt warming in the north (resumption of the circulation), CO_2 is decreasing again. This is in qualitative agreement with the information from the ice cores (Fig. 7) and lends further confidence in the hypothesis that the abrupt climate changes are due to changes in the Atlantic THC with associated far-field effects into the polar areas of the southern hemisphere.

4.2 A possible sequence of events during deglaciation

Based on the lessons from models and high-resolution paleoclimatic records, a sequence of events that characterised the last termination is proposed. Several observations need to be reconciled by such a scenario: the early warming recorded in Antarctica, the prolonged cold phase in Greenland up to the first abrupt temperature increase around 14.5 kyr BP, and the conspicuous sequence of Antarctic Cold Reversal (ACR) in the south and Younger Dryas in the north (Fig. 8).

We note that as soon as there is a strong warming in the north (14.5 kyr BP) the south stops warming and the ACR starts. At the same time, the north starts to cool down again over the next 1500 years during the Bølling/Allerød. The start of the YD cold event in the north coincides in time with the resumption of warming in the south which is, again, interrupted when YD terminates. This sequence strongly suggests the seesaw coupling coupling of northern and southern hemispheres during this sequence of abrupt climate change.

There is growing confusion with the notions "in phase" and "out of phase" or "antiphase" in the context of abrupt climate change. As evident from Fig. 6 and Fig. 8 one could argue that the warmest periods recorded in the Antarctic ice cores are in phase with the warmest peaks in the Greenland cores and hence, north and south are in phase. However, the warming in the south clearly starts during the phases of cold in the north, and reverses its trend about at the time the north warms abruptly. Subsequently, during the warm interstadials in the north, the souths slowly cools. This behaviour is predicted by the seesaw analogy (Fig. 5), and "antiphase" apprears to more clearly describe the characteristics of the record.

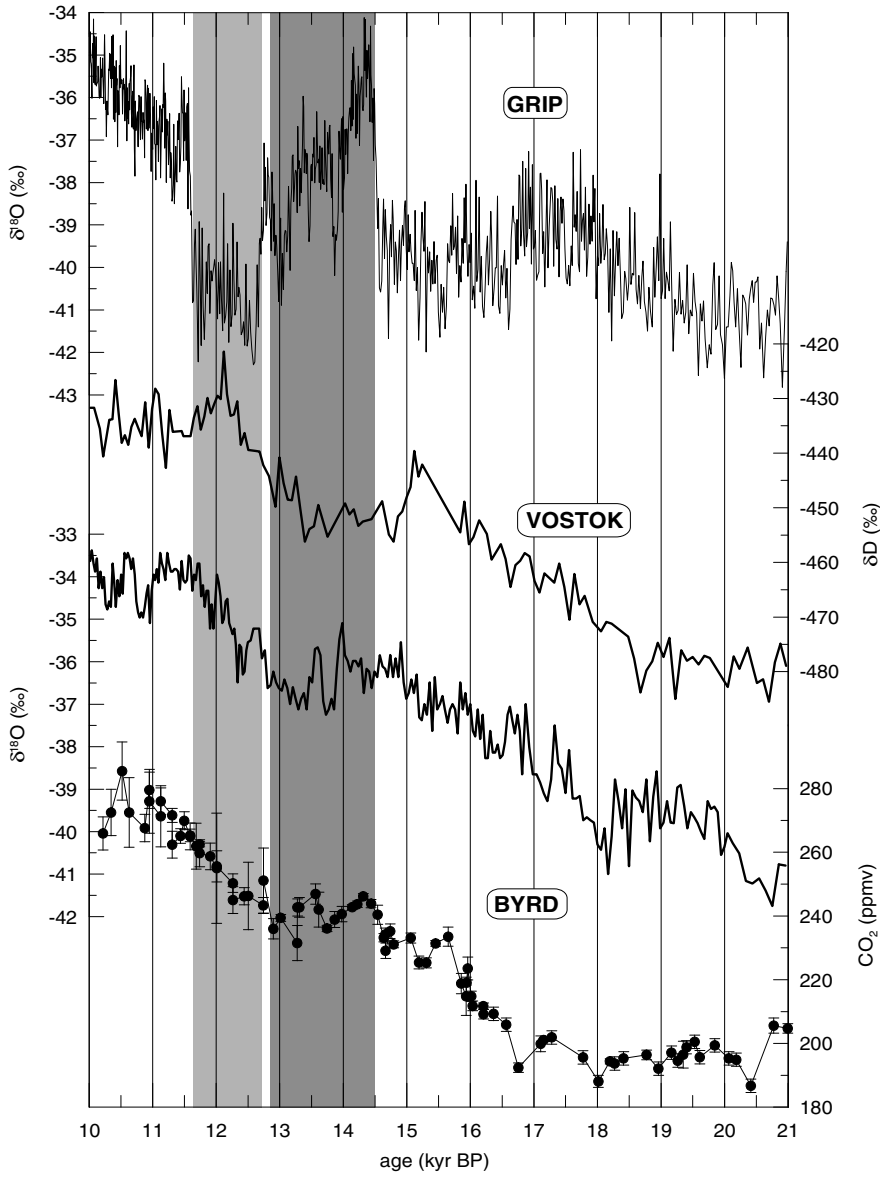

Figure 8: High-resolution climate records based on polar ice cores from Greenland and Antarctica during the last deglaciation from 21 to 10 kyr BP including a sequence of abrupt climate changes in the northern hemisphere. Changes in the isotopic composition of the water molecule, δ^{18}O and δD, indicate temperature variations. Atmospheric CO_2 is measured in bubbles enclosed in Antarctic ice from Byrd station (Blunier *et al.* 1997; Marchal *et al.* 1999) and increases almost linearly during Younger Dryas (YD). The increase is interrupted during the Antarctic Cold Reversal (strong shading). Deglaciation begins at around 21 kyr BP in both hemispheres but is interrupted in the north, likely due to Heinrich event 1 (16.5 kyr BP). The transition into the Bølling (strong shading) warm phase is abrupt and probably initiates the cooling in Antarctica (Antarctic Cold Reversal). This slight cold phase is interrupted when YD begins in the northern hemisphere at 12.7 kyr BP (weak shading).[Figure based on Blunier *et al.* 1997, reproduced from Stocker 2000]

Based on the paleoclimatic record, we speculate about possible sequences of events during deglaciation (Fig. 9). When deglaciation starts in response to changes in insolation around 19 kyr BP, a massive discharge of icebergs from the major ice sheets (H-event 1) occurs which shuts off the Atlantic THC and suppresses warming in the north until 14.5 kyr BP. Warming continues in the south unabated and meltwater is created there which influences

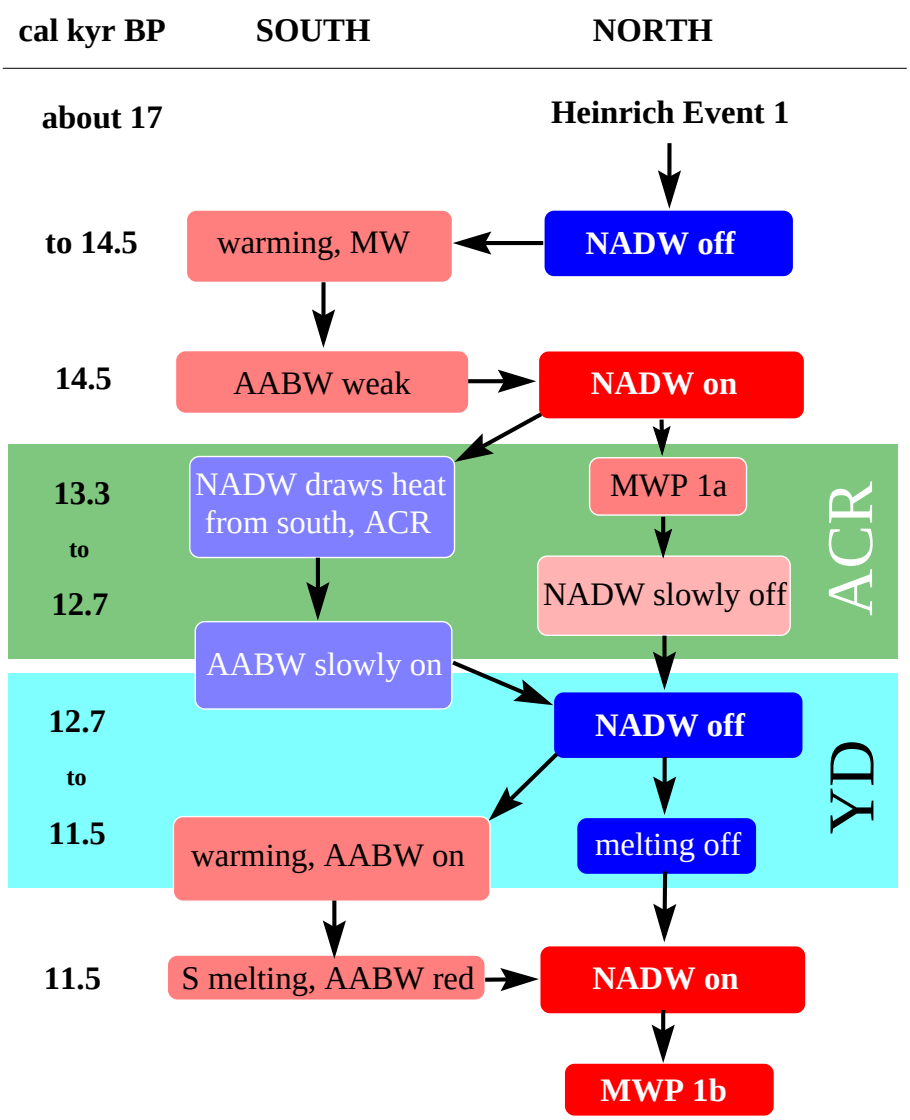

Figure 9: Schematics of the evolution and interaction between climatic events occurring in the southern hemisphere and those in the northern hemisphere. The central period of the last deglaciation from 14.5 to about 11.5 kyr BP comprises a series of abrupt changes that manifest the full dynamics of the climate system. The abbreviations MW (melt water), MWP (melt water peak), NADW (North Atlantic Deep Water), AABW (Antarctic Bottom Water), ACR (Antarctic Cold Reversal) and YD (Younger Dryas) are used. This schematics is inspired by recent results from synchronizing ice cores from Greenland and Antarctica (Blunier *et al.* 1997) as well as modeling simulations.

the density and the rate of water formation of southern origin. At a critical threshold, the Atlantic THC switches on and creates the sudden warming at 14.5 kyr BP. According to the heat flux argument (Crowley 1992), the south starts cooling and the ACR begins. On the other hand, the warming in the north promotes melting, and with a sequence of meltwater spikes, the THC decreases slowly and finally collapses to initiate the YD cooling event. Warming in the south can now resume and the same steps as after H-event 1 repeat.

It is clear that the proposed sequence is speculative. However, the paleoclimatic record and the few model simulations are consistent with this picture. Only high-resolution records that are temporally synchronised plus more comprehensive model simulations

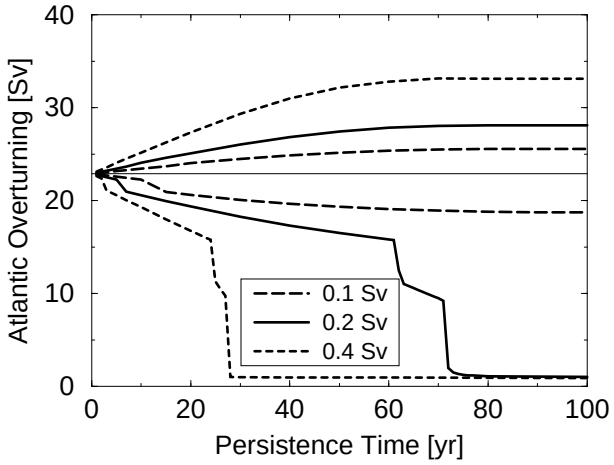

Figure 10: Changes in the Atlantic THC as a response to sustained tropical freshwater forcing associated with persistent El Niño (upper lines) or La Niña (lower lines) phases. For strong forcing the THC collapses if La Niña persists for several decades. [From (Schmittner *et al.* 2000)]

with provide us with a better check whether or not this scenario will survive.

4.3 High latitudes or tropics – or both ?

Classically, the high latitudes around the North Atlantic have been considered the center of action for abrupt change. They are attractive because most of the paleoclimatic evidence comes from this region, and these records indicate that amplitudes of changes are strongest there (e.g., 16°C changes in Greenland at the end of a typical D/O event, Lang *et al.* 1999). Furthermore, modeling suggests that the THC is not stable and that rapid coolings can be triggered by changes in the freshwater balance. Although there emerges quite a consistent picture, it is surprising that other, climatically important areas should not play a role in abrupt climate change. Interestingly, the simple mechanical analogue of the bipolar seesaw (Fig. 5) offers two alternate driving locations of the seesaw. The first, and classical location would be the high latitude, i.e. the forcing is where the strongest responses are expected (Fig. 5a). The second possibility is that an instability of the system is generated via changes at the fulcrum of the seesaw (Fig. 5b), i.e. at a point of minimum local response. By analogy, the seesaw points to the tropics!

The tropics are the Earth's heat engine and major supplier of water vapor, the most important greenhouse gas. It is where most of the energy from the Sun is taken up and redistributed in the climate system. The role of the low latitudes for the dynamics of abrupt change has hardly been investigated (Cane 1998). One low-latitude process with documented strong global teleconnections is El Niño/Southern Oscillation (ENSO). Temperature anomalies during a strong ENSO can easily reach 6°C as distant as Central North America (Cane 1998). ENSO also changes the surface freshwater balance of the Atlantic Ocean with about 0.1 Sv corresponding to a 2σ change in the Southern Oscillation Index (Schmittner *et al.* 2000). This gives rise to an interesting hypothesis: if the dynamical system of the tropical Pacific locked for some time into a specific phase, e.g. a persistent El Niño, what would be the effect of such a change on other components of the climate system?

Schmittner *et al.* (2000) used their simplified model to test this hypothesis. They found that if a very strong La Niña condition persisted for a few decades, this would be sufficient to collapse the Atlantic THC (Fig. 10). The simplified model therefore suggests an intriguing scenario: The abrupt changes that are recorded in the north might actually be the consequence of major changes in the tropical Pacific and the teleconnections that are established. While the model indicates a potentially important process, climate modelling is far from quantitatively testing this because of problems defining initial conditions (we do not know how close the atmosphere-ocean system was to a threshold during the glacial), and because comprehensive 3D models are only now beginning to simulate ENSO in a realistic way (Fedorov & Philander 2000).

Whether ENSO was present during the glacial or how ENSO was modified due to an altered seasonal cycle of solar radiation, different ocean bathymetry and large continental ice sheets is unknown. Simulations with simplified models suggest that ENSO was active with unaltered spatial structure but modified frequency (Clement *et al.* 1999; Liu *et al.* 2000).

5 Future Changes and Feedback Processes

5.1 Collapse of the Atlantic Thermohaline Circulation

Climate modelling suggests that the surface freshwater balance exerts a strong control on the THC in the North Atlantic (Manabe & Stouffer 1988; Stocker & Wright 1991a; Mikolajewicz & Maier-Reimer 1994) and that multiple equilibria can result (Fig. 4). In the glacial, ice sheets provided the perturbation mechanism: ice streams which surge into the Atlantic ocean may introduce enough freshwater to periodically disrupt the THC and trigger abrupt coolings. The last such event probably lead to the 8,200 yr BP cooling event (Barber *et al.* 1999; Alley *et al.* 1997; Leuenberger *et al.* 1999), but since the disintegration of all northern hemisphere ice sheets (except Greenland), such events have been absent.

However, this does not mean that the ocean-atmosphere system has now moved into a region of absolute stability. Warmer air temperatures, such as projected for the next century due to a continuing emission of greenhouse gases, are likely to enhance the hydrological cycle. This link between temperature and hydrological cycle is manifested by the methane changes during each D/O event: the warming is associated with a 50% increase in the CH_4 concentration whose source areas are the mid and high northern latitudes (Dällenbach *et al.* 2000). This is consistent with the notion that relatively warmer climate would cause a stronger meridional moisture transport.

In summary, warming would tend to strengthen evaporation at low latitudes, increase precipitation at higher latitudes and thus accelerate the hydrological cycle. As ocean models indicate, this would lead to a reduction of deep water formation in the northern North Atlantic due to a freshening of the surface waters. A reduction of sea surface density is also caused by the increased surface air temperatures further reducing the thermohaline circulation. While the relative strength of these two mechanisms is debated (Dixon *et al.* 1999; Mikolajewicz & Voss 2000), a general reduction of the Atlantic THC in response

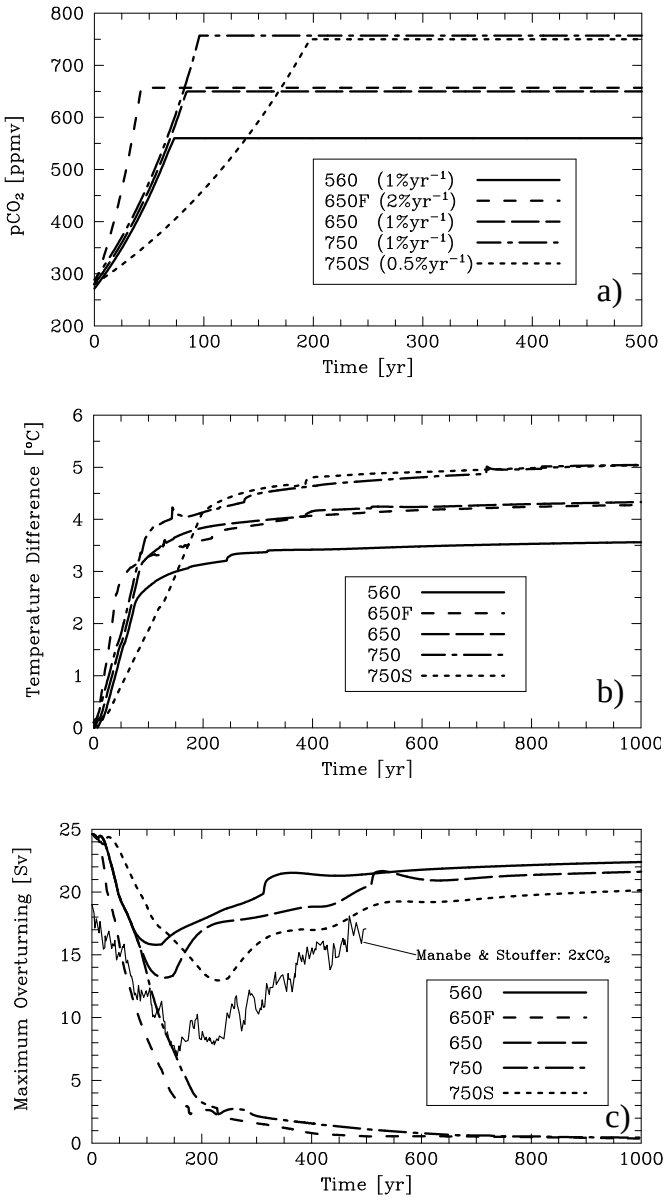

Figure 11: a: Prescribed evolution of atmospheric CO_2 for five global warming experiments. **b:** Simulated global mean surface air temperature changes. The climate sensitivity for a doubling of CO_2 was set at 3.7°C in agreement with the simulation of Manabe & Stouffer (1993). **c:** Evolution of the maximum meridional overturning of the North Atlantic in Sverdrup ($1\,\mathrm{Sv} = 10^6 \mathrm{m}^3/\mathrm{s}$). Note the good agreement between the overturning simulated in the simplified model with that of the 3D AOGCM. [modified from Stocker & Schmittner 1997]

to global warming appears to be a robust result found by the entire hierarchy of climate models (IPCC 2001).

As already Fig. 4 suggests, threshold values of key climate variables exist beyond which the THC can no longer be sustained. Among these are the level of greenhouse gases in the atmosphere (Manabe & Stouffer 1993) as well as the rate of increase of greenhouse gas concentration (Stocker & Schmittner 1997; Stouffer & Manabe 1999). This is illustrated in Fig. 11.The climate sensitivity is set at 3.7°C for a doubling of CO_2 in agreement with Manabe & Stouffer (1993). The standard rate of CO_2 increase is 1%/yr compounded;

experiments with a fast rate of 2%/yr (denoted F) and a slow rate of 0.5%/yr (denoted S) are also performed. The maximum CO_2 values are 560 ppmv (exp. 560), 650 ppmv for experiments 650 and 650F, and 750 ppmv for experiments 750 and 750S. Once the maximum value is reached, CO_2 is held constant (Fig. 11a).

Simulated global mean surface air temperature changes do not depend on the emission history for a given maximum CO_2 concentration (Fig. 11b). However, there exists a bifurcation point for the maximum meridional overturning of the North Atlantic (Fig. 11c). In all cases, a reduction is obtained with an amplitude depending on the values of maximum atmospheric CO_2 and of the rate of CO_2 increase. The circulation collapses permanently for a maximum concentration of 750 ppmv with an increase at a rate of 1%/yr (exp. 750). It recovers, however, and settles to a reduced value if the increase is slower (0.5%/yr, exp. 750S) or if the final CO_2 level is reduced to 650 ppmv (exp. 650). Similarly, for a fast increase (exp. 650F) at a rate of 2%/yr the circulation collapses. All experiments have been integrated for 10,000 years and no further changes have been observed. In other words, once the THC collapses it settles to a new equilibrium and changes are hence irreversible.

The few model simulations show, that the critical level for THC collapse is somewhere between double and fourfold preindustrial CO_2 concentration, but this depends critically on various model parameterizations (Schmittner & Stocker 1999; Knutti *et al.* 2000). The threshold lies lower if the CO_2 increase is faster. If the threshold is crossed, a complete collapse of the Atlantic THC ensues which results in regional cooling and water mass reorganization very similar to the paleoclimatic experiments with the same model.

Most 3-D simulations indicate a reduction of the THC by the year 2060, but not a complete collapse (IPCC 2001). A collapse appears therefore unlikely to occur by 2100 but it can not be ruled out for later. Important in this context is to note that a reduction of the THC moves the system closer to the threshold and the likelihood of a collapse may well increase (Tziperman 2000). Concern for this potentially irreversible phenomenon may thus increase in the future.

5.2 Impact of the Projected Sea Level Rise

The Atlantic THC is an important transport mechanism from the surface to the depth. The amount of heat mixed into the interior of the ocean therefore depends also on the strength of the THC. A stronger THC would represent a more efficient downward transport of heat. More than half of the projected sea level rise is due to the thermal expansion of the water column (IPCC 1996). Because the vertical distribution of excess heat affects sea level, changes of the THC have the potential to influence the rate of sea level rise as well as that achieved under equilibrium.

The simplified models allow us to construct a well-defined experiment, in which the ocean model is placed at a bifurcation point. Just beyond the bifurcation point the THC collapses, otherwise it recovers. The point is that the equilibrium global warming in these two simulations is nearly identical but the internal distribution of heat may differ substantially. This is shown in Fig. 12. Global mean warming is about 1.8°C with an equilibrium sea level rise of about 0.5 m if the THC continues (solid lines, Fig. 12). However, if the circulation collapses, the equilibrium sea level rise is about 0.7 m larger. When the THC

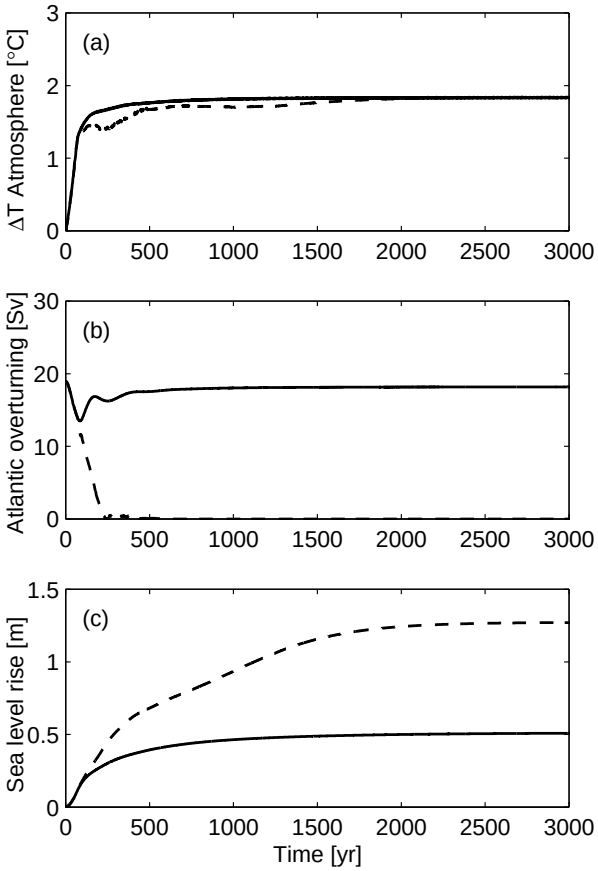

Figure 12: (a) Global mean atmospheric temperature increase, (b) Atlantic deep overturning, and (c) global mean sea level rise versus time in two almost identical global warming experiments using the model version with a Gent&McWilliams mixing scheme. If the Atlantic deep overturning collapses (dashed lines), steric sea level rise is much larger for the same atmospheric temperature increase than if the overturning recovers (solid lines). [From Knutti & Stocker 2000]

slows down, the surface waters in the North Atlantic tend to cool relative to a simulation in which the THC does not change. The increased air-sea temperature contrast therefore enhances the heat uptake during the transient phase.

5.3 A possible runaway greenhouse effect?

Given the insights about the workings of the climate system, we must pose a burning question: Do these massive ocean reorganisations have to potential to trigger a runaway greenhouse effect? The reasoning goes as follows (Fig. 13). A warming atmosphere clearly leads to increasing sea surface temperatures (SST) which, in turn, reduce the solubility of CO_2 in the surface waters. Warmer waters hold less dissolved carbon and warming thus causes an outgassing of this greenhouse gas. This constitutes a positive feedback loop (top in Fig. 13) enhancing the initial increase of atmospheric CO_2. A further positive feedback loop (left in Fig. 13) is associated with the effect of downward transport of carbon by the THC. If the THC collapses, much less carbon will be buried in the deep sea, again reinforcing accumulation of CO_2 in the atmosphere.

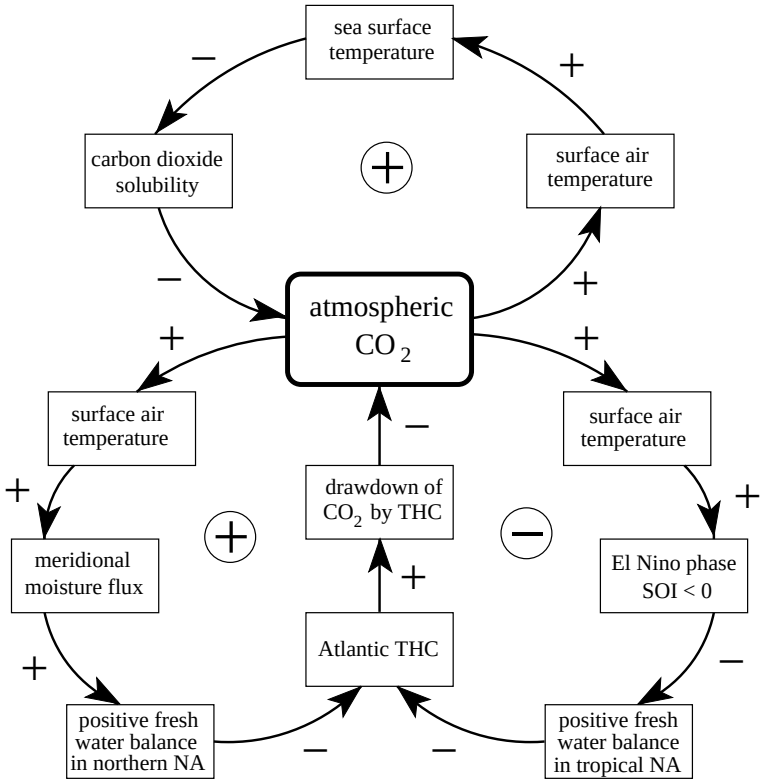

Figure 13: Possible feedback mechanisms that influence the atmospheric CO_2 concentration. In two cases, a positive feedback occurrs with the potential of reinfocing the warming. NA denotes North Atlantic, SOI is the Southern Oscillation Index.

There is a third feedback loop added in Fig. 13. It is based on previous experiments which point to a stabilising effect of possible changes in ENSO as explained in section 4.3. Notwithstanding, there seems enough concern to use physical-biogeochmical models to investigate quantitatively the question, how much these positive feedback mechanisms could contributed to an increase in atmospheric CO_2.

Model simulations using 3-dimensional ocean general circulation models with prescribed boundary conditions predicted a minor (Maier-Reimer *et al.* 1996) or a rather strong (Sarmiento & Le Quéré 1996) feedback between the circulation changes and the uptake of anthropogenic CO_2 under global warming scenarios. However, the complete interplay of the relevant climate system and carbon cycle components was only taken into account in the recent study by Joos *et al.* (1999). A series of CO_2 stabilization profiles were prescribed for the next 500 years along with a specific climate sensitivity, i.e. the global mean temperature increase due to a doubling of CO_2: typically 1.5–4.5°C (Fig. 14a). As expected this leads to a reduction of the Atlantic THC. Again, a threshold value is between 750 and 1000 ppmv for a complete cessation of the THC (Fig. 14b).

With this model different experiments with the ocean carbon pumps operating or suppressed can be performed. Such experiments are essential for a better understanding of the various processes influencing ocean uptake of CO_2 and shown in Fig. 15. A maximum uptake of 5.5 Gt/yr is simulated if there is no change in ocean circulation nor sea surface temperature (curve A). The full simulation including all feedbacks (sea surface temperature, circulation and biota) shows a long-term reduction of almost 50% in the uptake

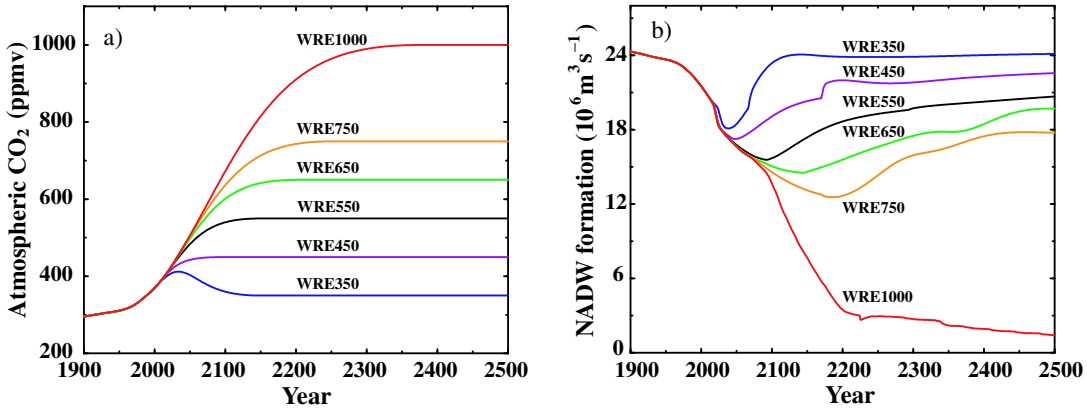

Figure 14: (a) Scenarios for the stabilization of atmospheric CO_2 concentration over the next 500 years; (b) evolution of the overturning circulation in the Atlantic in response to global warming caused by increasing concentration of CO_2. The climate sensitivity of the current experiments is 3.7°C for a doubling of CO_2 [From Joos *et al.* 1999].

flux provided the Atlantic THC collapses (curve B). The solubility effect is important in the first 100 years (curve C) but later, the circulation effect takes over (curve D). If the circulation does not break down as in WRE550 (Fig. 15b), circulation and biota feedback compensate each other, and the solubility effect remains the only significant feedback effect. The reduction of strength of the ocean as a major carbon sink appears a robust result, but the model also shows that dramatic feedback effects (such as a runaway greenhouse effect) are very unlikely. The maximum increase of CO_2 in the case of a collapsed Atlantic THC is estimated at about 20%. This result is entirely consistent with the evidence from the paleoclimatic records: major atmosphere-ocean reorganizations such as expected during H- or D/O-events appeared to have a relatively small influence on atmospheric CO_2 equivalent to about 30 ppm at most.

6 Conclusions

Important aspects of climate change, in particular the series of abrupt changes during the last glacial and the sequence of events that characterised the last transition from the glacial to the present warm period, are determined by chagnes in the deep circulation of the ocean. Abrupt warmings and cooling, and their counterparts in the southern hemeisphere can be explained by the operation of the Atlantic thermohaline circulation. Models suggest that this circulation is vulnerable to changes in the surface freshwater balance. Ice sheets have presented important sources of perturbations to the freshwater balance in the Atlantic. Frequent discharges of icebergs, which introduce massive amounts of freshwater upon melting, are recorded in marine sediments as so-called Heinrich layers. Major climatic changes are recorded in the Greenland ice cores and other high-resolution archivews around the time of these Heinrich events. Simplified models, particularly when coupled to components of biogeochemical cycles, provide a framework to study in detail the processes that are responsible for these climatic changes.

The same models also make predictions for the future. In a warmer world, the surface

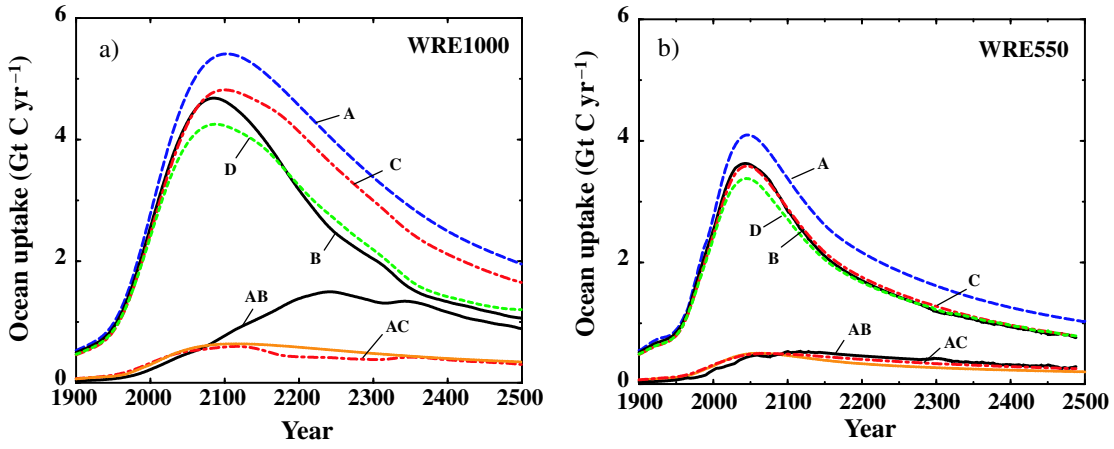

Figure 15: Evolution of the oceanic uptake of carbon dioxide for the different stabilization scenarios of Fig. 14. In WRE1000 (a), the Atlantic thermohaline circulation collapses completely by year 2500, in WRE550 (b) it remains close to the initial strength. The different simulations are labelled A–D. In A, all feedbacks are neglected (constant ocean), B is the full simulation (temperature, circulation, biota changes), C is only sea surface temperature changes (circulation held constant), D (temperature and circulation changes). Further explanations on regarding the different scenarios are in the text [From Joos *et al.* 1999].

freshwater balance of the Atlantic will most likely be altered. Models suggest that the changes are towards more freshwater due to an enhanced meridional transport of freshwater. The thermohaline circulation reacts in the same way as it did to the iceberg perturbation: the THC reduces, in some simulations it even stops. Such changes would be massive and, although not very likely to occurr in this century, would have a profound impact on all aspects of climate, especially in the North Atlantic region. Furthermore, the same models indicate that the reduction of the THC itself moves the system closer to thresholds and instability becomes more likely.

A key task of climate research is therefore a detailed exploration of the state of the ocean-atmosphere system in order to answer the following questions:

- Is there evidence for rapid changes in warmer climates?
- What is the current state of the ocean circulation?
- Which are the thresholds and how close is the ocean-atmosphere system to them?
- How fast in in which direction is the system evolving with respect to these thresholds?

It is clear that only a very close collaboration between paleoclimatic research, observational studies in key areas and modelling using a hierarchy ranging from simplified dynamical models to 3-dimensional coupled general circulation models of the highest resolution will have the change of providing answers to these pressing questions.

Acknowledgment: The style of this article is far away from what I have learned 15 years ago during my PhD studies with Kolumban Hutter. Nevertheless intricate equations and their solutions are still at the heart of any climate model, even the simplified described in this contribution. I am very grateful to Kolumban for the fruitful years we worked together. They way he supported, motivated, and sometimes pushed his students, will always be remembered fondly.

References

Alley, R. B. (2000). ice-core evidence of abrupt cliamte change. *Proc. US Natl. Acad. Sci. 97*, 1331–1334.

Alley, R. B., P. A. Mayewski, T. Sowers, M. Stuiver, K. C. Taylor, & P. U. Clark (1997). Holocene climatic instability: A prominent, widespread event 8200 yr ago. *Geology 25*, 483–486.

Barber, D. C., A. Dyke, C. Hillaire-Marcel, A. E. Jennings, J. T. Andrews, M. W. Kerwin, G. Bilodeau, R. McNeely, J. Southon, M. D. Morehead, & J.-M. Gagnon (1999). Forcing of the cold event of 8,200 years ago by catastrophic drainage of Laurentide lakes. *Nature 400*, 344–348.

Blunier, T. *et al.* (1997). Timing of temperature variations during the last deglaciation in Antarctica and the atmospheric CO_2 increase with respect to the Younger Dryas event. *Geophys. Res. Let. 24*, 2683–2686.

Blunier, T., J. Chappellaz, J. Schwander, A. Dällenbach, B. Stauffer, T. F. Stocker, D. Raynaud, J. Jouzel, H. B. Clausen, C. U. Hammer, & S. J. Johnsen (1998). Asynchrony of Antarctic and Greenland climate change during the last glacial period. *Nature 394*, 739–743.

Blunier, T., J. Schwander, B. Stauffer, T. Stocker, A. Dällenbach, A. Indermühle, J. Tschumi, J. Chappellaz, D. Raynaud, & J.-M. Barnola (1997). Timing of temperature variations during the last deglaciation in Antarctica and the atmospheric CO_2 increase with respect to the Younger Dryas event. *Geophys. Res. Let. 24*, 2683–2686.

Bond, G. C. & R. Lotti (1995). Iceberg discharges into the North Atlantic on millennial time scales during the last glaciation. *Science 267*, 1005–1010.

Böning, C., F. O. Bryan, W. R. Holland, & R. Döscher (1996). Deep-water formation and meridional overturning in a high-resolution model of the North Atlantic. *J. Phys. Oceanogr. 26*, 1142–1164.

Broecker, W. S. (1987). The biggest chill. *Natural Hist. 96*, 74–82.

Broecker, W. S. (1991). The great ocean conveyor. *Oceanography 4*, 79–89.

Broecker, W. S. (1998). Paleocean circulation during the last deglaciation: a bipolar seesaw? *Paleoceanogr. 13*, 119–121.

Broecker, W. S., D. M. Peteet, & D. Rind (1985). Does the ocean-atmosphere system have more than one stable mode of operation? *Nature 315*, 21–25.

Bryan, F. (1986). High-latitude salinity effects and interhemispheric thermohaline circulations. *Nature 323*, 301–304.

Budyko, M. I. (1969). The effect of solar radiation variations on the climate of the earth. *Tellus 21*, 611–619.

Cane, M. A. (1998). A role for the tropics. *Science 282*, 59–61.

Chappellaz, J., T. Blunier, D. Raynaud, J. M. Barnola, J. Schwander, & B. Stauffer (1993). Synchronous changes in atmospheric CH_4 and Greenland climate between 40 and 8 kyr BP. *Nature 366*, 443–445.

Claussen, M., C. Kubatzki, V. Brovkin, A. Ganopolski, P. Hoelzmann, & H. Pachur (1999). Simulation of an abrupt change in Saharan vegetation in the mid-Holocene. *Geophys. Res. Let. 26*, 2037–2040.

Clement, A., R. Seager, & M. Cane (1999). Orbital controls on the El Niño/Southern Oscillation and the tropical climate. *Paleoceanogr. 14*, 441–455.

Crowley, T. J. (1992). North Atlantic deep water cools the southern hemisphere. *Paleoceanogr. 7*, 489–497.

Crowley, T. J. & S. K. Baum (1997). Effect of vegetation on an ice-age climate model simulation. *J. Geophys. Res. 102*, 16463–16480.

Crowley, T. J. & G. R. North (1991). *Paleoclimatology*. Number 18 in Oxford Monographs on Geology and Geophysics. Oxford University Press. 339 pp.

Dällenbach, A., T. Blunier, J. Flückiger, B. Stauffer, J. Chappellaz, & D. Raynaud (2000). Changes in the atmospheric CH_4 gradient between Greenland and Antarctica during the Last Glacial and the transition to the Holocene. *Geophys. Res. Let. 27*, 1005–1008.

Dansgaard, W., S. J. Johnsen, H. B. Clausen, D. Dahl-Jensen, N. S. Gundestrup, C. U. Hammer, C. S. Hvidberg, J. P. Steffensen, A. E. Sveinbjornsdottir, J. Jouzel, & G. Bond (1993). Evidence for general instability of past climate from a 250-kyr ice-core record. *Nature 364*, 218–220.

de Ruijter, W. P. M., A. Biastoch, S. S. Drijfhout, J. R. E. Lutjeharms, R. P. Matano, T. Pichevin, P. J. van Leeuwen, & W. Weijer (1998). Indian-Atlantic interocean exchange: Dynamics, estimation and impact. *J. Geophys. Res. 104*, 20885–20910.

Dixon, K. W., T. L. Delworth, M. J. Spelman, & R. J. Stouffer (1999). The influence of transient surface fluxes on North Atlantic overturning in a coupled GCM climate change experiment. *Geophys. Res. Let. 26*, 2749–2752.

Fedorov, A. V. & S. G. Philander (2000). Is El Niño changing? *Science 288*, 1997–2002.

Galleé, H., J. P. Van Ypersele, T. Fichefet, C. Tricot, & A. Berger (1991). Simulation of the last glacial cycle by a coupled, sectorially averaged climate-ice sheet model. 1. the climate model. *J. Geophys. Res. 96*, 13139–13161.

Ganopolski, A., S. Rahmstorf, V. Petoukhov, & M. Claussen (1998). Simulation of modern and glacial climates with a coupled global model of intermediate complexity. *Nature 391*, 351–356.

Gill, A. E. (1982). *Atmosphere-Ocean Dynamics*, Volume 30 of *Int. Geophys. Ser.* Academic, San Diego, Calif. 662 pp.

Gordon, A. L. (1986). Interocean exchange of thermocline water. *J. Geophys. Res. 91*, 5037–5046.

Hall, M. M. & H. L. Bryden (1982). Direct estimates and mechanisms of ocean heat transport. *Deep Sea Res. 29*, 339–359.

Heinrich, H. (1988). Origin and consequences of cyclic ice rafting in the Northeast Atlantic Ocean during the past 130,000 years. *Quat. Res. 29*, 142–152.

Indermühle, A., E. Monnin, B. Stauffer, T. F. Stocker, & M. Wahlen (2000). Atmospheric CO_2 concentration from 60 to 20 kyr BP from the Taylor Dome ice core, Antarctica. *Geophys. Res. Let. 27*, 735–738.

IPCC (1996). *Climate Change 1995, The Science of Climate Change*. Intergovernmental Panel on Climate Change, Cambridge University Press. 572 pp.

IPCC (2001). *Climate Change 2001: The Scientific Basis. Contribution of Working Group I to the Third Assessment Report of of the Intergovernmental Panel on Climate Change*. Intergovernmental Panel on Climate Change, Cambridge University Press. 881 pp.

Joos, F., G.-K. Plattner, T. F. Stocker, O. Marchal, & A. Schmittner (1999). Global warming and marine carbon cycle feedbacks on future atmospheric CO_2. *Science 284*, 464–467.

Knutti, R. & T. F. Stocker (2000). Influence of the thermohaline circulation on projected sea level rise. *J. Clim. 13*, 1997–2001.

Knutti, R., T. F. Stocker, & D. G. Wright (2000). The effects of sub-grid-scale parameterizations in a zonally averaged ocean model. *J. Phys. Oceanogr. 30*, 2738–2752.

Lang, C., M. Leuenberger, J. Schwander, & S. Johnsen (1999). 16°C rapid temperature variation in Central Greenland 70,000 years ago. *Science 286*, 934–937.

Leuenberger, M., C. Lang, & J. Schwander (1999). δ^{15}N measurements as a calibration tool for the paleothermometer and gas-ice age differences. A case study for the 8200 B.P. event on GRIP ice. *J. Geophys. Res. 104*, 22163–22170.

Liu, Z., J. Kutzbach, & L. Wu (2000). Modeling climate shift of El Niño variability in the Holocene. *Geophys. Res. Let. 27*, 2269–2272.

MacAyeal, D. R. (1993). A low-order model of the Heinrich event cycle. *Paleoceanogr. 8*, 767–773.

Macdonald, A. M. & C. Wunsch (1996). An estimate of global ocean circulation and heat fluxes. *Nature 382*, 436–439.

Maier-Reimer, E., U. Mikolajewicz, & A. Winguth (1996). Future ocean uptake of CO_2: interaction between ocean circulation and biology. *Clim. Dyn. 12*, 711–721.

Manabe, S. & R. J. Stouffer (1988). Two stable equilibria of a coupled ocean-atmosphere model. *J. Clim. 1*, 841–866.

Manabe, S. & R. J. Stouffer (1993). Century-scale effects of increased atmospheric CO_2 on the ocean-atmosphere system. *Nature 364*, 215–218.

Manabe, S. & R. J. Stouffer (1997). Coupled ocean-atmosphere model response to freshwater input: comparison to Younger Dryas event. *Paleoceanogr. 12*, 321–336.

Marchal, O., R. François, T. F. Stocker, & F. Joos (2000). Ocean thermohaline circulation and sedimentary $^{231}Pa/^{230}Th$ ratio. *Paleoceanogr. 15*, 625–641.

Marchal, O., T. F. Stocker, & F. Joos (1998). Impact of oceanic reorganizations on the ocean carbon cycle and atmospheric carbon dioxide content. *Paleoceanogr. 13*, 225–244.

Marchal, O., T. F. Stocker, F. Joos, A. Indermühle, T. Blunier, & J. Tschumi (1999). Modelling the concentration of atmospheric CO_2 during the Younger Dryas climate event. *Clim. Dyn. 15*, 341–354.

Marotzke, J. (1990). *Instabilities and Multiple Equilibria of the Thermohaline Circulation*. Ph. D. thesis, Christian-Albrechts-Universität Kiel. 126 pp.

Marotzke, J., P. Welander, & J. Willebrand (1988). Instability and multiple equilibria in a meridional-plane model of the thermohaline circulation. *Tellus 40A*, 162–172.

Marshall, J. & F. Schott (1999). Open-ocean convection: observations, theory and models. *Rev. Geophys. 37*, 1–64.

Mikolajewicz, U. & E. Maier-Reimer (1994). Mixed boundary conditions in ocean general circulation models and their influence on the stability of the model's conveyor belt. *J. Geophys. Res. 99*, 22633–22644.

Mikolajewicz, U. & R. Voss (2000). The role of the individual air-sea flux components in CO_2-induced changes of the ocean's circulation and climate. *Clim. Dyn. 16*, 627–642.

North, G. R., R. F. Cahalan, & J. A. Coakley (1981). Energy balance climate models. *Rev. Geophys. Space Phys. 19*, 91–121.

Pedlosky, J. (1996). *Ocean Circulation Theory*. Springer. 453 pp.

Petoukhov, V., A. Ganopolski, V. Brovkin, M. Claussen, A. Eliseev, C. Kubatzki, & S. Rahmstorf (2000). CLIMBER-2: a climate system model of intermediate complexity. Part I: model description and performance for present climate. *Clim. Dyn. 16*, 1–17.

Quon, C. & M. Ghil (1994). Multiple equilibria and stable oscillations in thermosolutal convection at small aspect ratio. *J. Fluid Mech. 291*, 35–56.

Rahmstorf, S. (1995). Bifurcations of the Atlantic thermohaline circulation in response to changes in the hydrological cycle. *Nature 378*, 145–149.

Rooth, C. (1982). Hydrology and ocean circulation. *Prog. Oceanogr. 11*, 131–149.

Sachs, J. P. & S. J. Lehman (1999). Subtropical North Atlantic temperatures 60,000 to 30,000 years ago. *Science 286*, 756–759.

Saravanan, R. & J. C. McWilliams (1995). Multiple equilibria, natural variability, and climate transitions in an idealized ocean–atmosphere model. *J. Clim. 8*, 2296–2323.

Sarmiento, J. L. & C. Le Quéré (1996). Oceanic carbon dioxide in a model of century-scale global warming. *Science 274*, 1346–1350.

Schiller, A., U. Mikolajewicz, & R. Voss (1997). The stability of the North Atlantic thermohaline circulation in a coupled ocean-atmosphere general circulation model. *Clim. Dyn. 13*, 325–347.

Schmittner, A., C. Appenzeller, & T. F. Stocker (2000). Enhanced Atlantic freshwater export during El Niño. *Geophys. Res. Let. 27*, 1163–1166.

Schmittner, A. & T. F. Stocker (1999). The stability of the thermohaline circulation in global warming experiments. *J. Clim. 12*, 1117–1133.

Schmittner, A. & T. F. Stocker (2001). A seasonally forced ocean-atmosphere model for paleoclimate studies. *J. Clim. 14*, 1055–1068.

Schmitz, W. J. (1995). On the interbasin-scale thermohaline circulation. *Rev. Geophys. 33*, 151–173.

Sellers, W. D. (1969). A global climate model based on the energy balance of the earth-atmosphere system. *J. Appl. Meteorol. 8*, 392–400.

Stauffer, B., T. Blunier, A. Dällenbach, A. Indermühle, J. Schwander, T. F. Stocker, J. Tschumi, J. Chappellaz, D. Raynaud, C. U. Hammer, & H. B. Clausen (1998). Atmospheric CO_2 and millennial-scale climate change during the last glacial period. *Nature 392*, 59–62.

Stocker, T. F. (1998). The seesaw effect. *Science 282*, 61–62.

Stocker, T. F. (1999). Climate changes: from the past to the future – a review. *Int. J. Earth Sci. 88*, 365–374.

Stocker, T. F. (2000). Past and future reorganisations in the climate system. *Quat. Sci. Rev. 19*, 301–319.

Stocker, T. F. & O. Marchal (2000). Abrupt climate change in the computer: is it real? *Proc. US Natl. Acad. Sci. 97*, 1362–1365.

Stocker, T. F. & A. Schmittner (1997). Influence of CO_2 emission rates on the stability of the thermohaline circulation. *Nature 388*, 862–865.

Stocker, T. F. & D. G. Wright (1991a). Rapid transitions of the ocean's deep circulation induced by changes in surface water fluxes. *Nature 351*, 729–732.

Stocker, T. F. & D. G. Wright (1991b). A zonally averaged model for the thermohaline circulation. Part II: Interocean exchanges in the Pacific-Atlantic basin system. *J. Phys. Oceanogr. 21*, 1725–1739.

Stocker, T. F. & D. G. Wright (1996). Rapid changes in ocean circulation and atmospheric radiocarbon. *Paleoceanogr. 11*, 773–796.

Stocker, T. F., D. G. Wright, & W. S. Broecker (1992). The influence of high-latitude surface forcing on the global thermohaline circulation. *Paleoceanogr. 7*, 529–541.

Stocker, T. F., D. G. Wright, & L. A. Mysak (1992). A zonally averaged, coupled ocean-atmosphere model for paleoclimate studies. *J. Clim. 5*, 773–797.

Stommel, H. (1948). The westward intensification of wind-driven ocean currents. *Trans. Am. Geophys. Union 29*, 202–206.

Stommel, H. (1958). The abyssal circulation. *Deep Sea Res. 5*, 80–82.

Stommel, H. (1961). Thermohaline convection with two stable regimes of flow. *Tellus 13*, 224–241.

Stommel, H. & A. B. Arons (1960). On the abyssal circulation of the world ocean - I. Stationary planetary flow patterns on a sphere. *Deep Sea Res. 6*, 140–154.

Stouffer, R. J. & S. Manabe (1999). Response of a coupled ocean-atmosphere model to increasing atmospheric carbon dioxide: sensitivity to the rate of increase. *J. Clim. 12*, 2224–2237.

Trenberth, K. E. & A. Solomon (1994). The global heat balance: heat transports in the atmosphere and ocean. *Clim. Dyn. 10*, 107–134.

Tziperman, E. (2000). Proximity of the present-day thermohaline circulation to an instability threshold. *J. Phys. Oceanogr. 30*, 90–104.

Warren, B. A. (1981). Deep circulation of the world ocean. In B. A. Warren & C. Wunsch (Eds.), *Evolution of Physical Oceanography – Scientific Surveys in Honor of Henry Stommel*, pp. 6–41. MIT Press.

Wright, D. G. & T. F. Stocker (1991). A zonally averaged ocean model for the thermohaline circulation, Part I: Model development and flow dynamics. *J. Phys. Oceanogr. 21*, 1713–1724.

Wright, D. G. & T. F. Stocker (1992). Sensitivities of a zonally averaged global ocean circulation model. *J. Geophys. Res. 97*, 12,707–12,730.

Wright, D. G., T. F. Stocker, & D. Mercer (1998). Closures used in zonally averaged ocean models. *J. Phys. Oceanogr. 28*, 791–804.